AFRL-OSR-VA-TR-2015-0150

Magnetospheric control of density and composition in the polar ionosphere

Joshua Semeter
TRUSTEES OF BOSTON UNIVERSITY

06/24/2015
Final Report

Air Force Research Laboratory
AF Office Of Scientific Research (AFOSR)/ RTB
Arlington, Virginia 22203
Air Force Materiel Command

REPORT DOCUMENTATION PAGE

Form Approved
OMB No. 0704-0188

1. REPORT DATE *(DD-MM-YYYY)*
13-06-2015

2. REPORT TYPE
Final Report

3. DATES COVERED *(From - To)*
April 2012 - March 2015

4. TITLE AND SUBTITLE
Magnetospheric control of density and composition in the polar ionosphere

5a. CONTRACT NUMBER

5b. GRANT NUMBER
FA9550-12-1-0184

5c. PROGRAM ELEMENT NUMBER

5d. PROJECT NUMBER

5e. TASK NUMBER

5f. WORK UNIT NUMBER

6. AUTHOR(S)
Joshua Semeter

7. PERFORMING ORGANIZATION NAME(S) AND ADDRESS(ES)
Boston University
8 Saint Mary's St.
Boston, MA 02215

8. PERFORMING ORGANIZATION REPORT NUMBER

9. SPONSORING/MONITORING AGENCY NAME(S) AND ADDRESS(ES)
Air Force Office of Science and Research
875 Randolph Street
Suite 325 Room 3112
Arlington, VA 22203

10. SPONSOR/MONITOR'S ACRONYM(S)
AFOSR

11. SPONSOR/MONITOR'S REPORT NUMBER(S)

12. DISTRIBUTION/AVAILABILITY STATEMENT
Approved for public release

13. SUPPLEMENTARY NOTES

14. ABSTRACT
This research has used collaborative observations by UHF incoherent scatter radar (ISR), the SuperDARN HF radar network, and wide-angle monochromatic optical imagers, supported by first-principles numerical modeling, to investigate the structure and composition of Earth's polar ionosphere. Key observational evidence has been provided by the electronically steerable Incoherent Scatter Radar at Resolute Bay, Canada. Findings include technical contributions related to the application of phased array ISR in the deep polar cap, as well as scientific contributions arising from the application of these techniques: 1) Development of a sensor fusion framework for combining simultaneous observations of auroral phenomena observed by radar and optical means [Semeter and Zettergren, 2014], 2) Development of a deconvolution approach for analyzing volumetric ISR measurements in a temporally and spatially varying ionosphere [Swoboda et al., 2015], 3) Discovery of direct evidence for internal structuring of convecting plasma patches [Dahlgren et al., 2013], 4) Quantitative description of electrodynamic coupling within polar auroral arcs developing along the nightside polar cap boundary [Perry et al., 2015], 5) Steepening of ionospheric density gradients via

15. SUBJECT TERMS
magnetosphere-ionosphere coupling, geospace, polar ionosphere, aurora, satellite drag, GNSS, scintillation

16. SECURITY CLASSIFICATION OF: a. REPORT	b. ABSTRACT	c. THIS PAGE	17. LIMITATION OF ABSTRACT	18. NUMBER OF PAGES	19a. NAME OF RESPONSIBLE PERSON
Unclassified	Unclassified	Unclassified	UU	10	Joshua Semeter

19b. TELEPHONE NUMBER *(Include area code)*
(617) 358-3498

Reset

INSTRUCTIONS FOR COMPLETING SF 298

1. REPORT DATE. Full publication date, including day, month, if available. Must cite at least the year and be Year 2000 compliant, e.g. 30-06-1998; xx-06-1998; xx-xx-1998.

2. REPORT TYPE. State the type of report, such as final, technical, interim, memorandum, master's thesis, progress, quarterly, research, special, group study, etc.

3. DATES COVERED. Indicate the time during which the work was performed and the report was written, e.g., Jun 1997 - Jun 1998; 1-10 Jun 1996; May - Nov 1998; Nov 1998.

4. TITLE. Enter title and subtitle with volume number and part number, if applicable. On classified documents, enter the title classification in parentheses.

5a. CONTRACT NUMBER. Enter all contract numbers as they appear in the report, e.g. F33615-86-C-5169.

5b. GRANT NUMBER. Enter all grant numbers as they appear in the report, e.g. AFOSR-82-1234.

5c. PROGRAM ELEMENT NUMBER. Enter all program element numbers as they appear in the report, e.g. 61101A.

5d. PROJECT NUMBER. Enter all project numbers as they appear in the report, e.g. 1F665702D1257; ILIR.

5e. TASK NUMBER. Enter all task numbers as they appear in the report, e.g. 05; RF0330201; T4112.

5f. WORK UNIT NUMBER. Enter all work unit numbers as they appear in the report, e.g. 001; AFAPL30480105.

6. AUTHOR(S). Enter name(s) of person(s) responsible for writing the report, performing the research, or credited with the content of the report. The form of entry is the last name, first name, middle initial, and additional qualifiers separated by commas, e.g. Smith, Richard, J, Jr.

7. PERFORMING ORGANIZATION NAME(S) AND ADDRESS(ES). Self-explanatory.

8. PERFORMING ORGANIZATION REPORT NUMBER. Enter all unique alphanumeric report numbers assigned by the performing organization, e.g. BRL-1234; AFWL-TR-85-4017-Vol-21-PT-2.

9. SPONSORING/MONITORING AGENCY NAME(S) AND ADDRESS(ES). Enter the name and address of the organization(s) financially responsible for and monitoring the work.

10. SPONSOR/MONITOR'S ACRONYM(S). Enter, if available, e.g. BRL, ARDEC, NADC.

11. SPONSOR/MONITOR'S REPORT NUMBER(S). Enter report number as assigned by the sponsoring/ monitoring agency, if available, e.g. BRL-TR-829; -215.

12. DISTRIBUTION/AVAILABILITY STATEMENT. Use agency-mandated availability statements to indicate the public availability or distribution limitations of the report. If additional limitations/ restrictions or special markings are indicated, follow agency authorization procedures, e.g. RD/FRD, PROPIN, ITAR, etc. Include copyright information.

13. SUPPLEMENTARY NOTES. Enter information not included elsewhere such as: prepared in cooperation with; translation of; report supersedes; old edition number, etc.

14. ABSTRACT. A brief (approximately 200 words) factual summary of the most significant information.

15. SUBJECT TERMS. Key words or phrases identifying major concepts in the report.

16. SECURITY CLASSIFICATION. Enter security classification in accordance with security classification regulations, e.g. U, C, S, etc. If this form contains classified information, stamp classification level on the top and bottom of this page.

17. LIMITATION OF ABSTRACT. This block must be completed to assign a distribution limitation to the abstract. Enter UU (Unclassified Unlimited) or SAR (Same as Report). An entry in this block is necessary if the abstract is to be limited.

Magnetospheric control of density and composition in the polar ionosphere

FINAL REPORT

Grant #: FA9550-12-1-0184

PI: Joshua Semeter, Boston University

Program Manager:

Dr. Kent Miller
Physics and Electronics Directorate
Space Sciences
AFOSR/RTB
kent.miller.2@us.af.mil

1 Executive Summary

Ionospheric variability is a critical consideration for communication systems, GNSS, and space asset management. At high magnetic latitudes, the convergent magnetic field acts as a lens, focusing electromagnetic power originating from solar wind-magnetosphere interactions into a limited latitudinal range. The geometry and ensuing complex coupling processes result in extreme multi-scale time-dependent variations in the structure and composition of the ionized gases in Earth's outer atmosphere. Understanding the mechanisms and technological consequences of these interactions benefits from distributed heterogeneous time-dependent measurements of the ionosphere-thermosphere-magnetosphere system, and their application as constraints on predictive space weather models.

This research used collaborative observations by UHF incoherent scatter radar (ISR), the HF SuperDARN radar network, and wide-angle optical imagers, supported by first-principles numerical modeling, to clarify the driving mechanisms and physical consequences of these interactions. Critical new observational evidence has been provided by the electronically steerable Resolute Bay Incoherent Scatter Radar (RISR, 74.7°N, 94.8°W), which has introduced a radically new sensing capability to polar ionospheric science. The results of this research include both technical contributions related to the application of phased array ISR in the polar cap, and scientific contributions arising from the application of these techniques. The major published results may be summarized as follows:

1) Development of a mathematical framework and software toolset for fusing optical imagery with three-dimensional ionospheric imagery derived from multi-beam ISR experiments [*Semeter and Zettergren*, 2014].
2) Development of a deconvolution framework for analyzing volumetric ISR measurements in a spatially and temporally varying ionosphere. The approach takes advantage of the observing flexibility of electronically steerable ISR to perform signal integration in the rest frame of a convecting plasma patch [*Swoboda et al.*, 2015].
3) Discovery of direct evidence for internal structuring of convecting polar plasma patches [*Dahlgren et al.*, 2012a].
4) Quantitative description of electrodynamic coupling within polar auroral arcs produced along the nightside polar cap boundary [*Perry et al.*, 2015].
5) Steepening of ionospheric density gradients via magnetosphere-ionosphere at the poleward auroral boundary [*Semeter et al.*, 2014].
6) Measurements of collisionless ion heating by Langmuir turbulence, related to soft particle fluxes in the aurora – a possible important "hidden" energy source in the F-region [*Akbari et al.*, 2015; *Akbari and Semeter*, 2014].

The software toolset developed under this grant enables routine analysis of common volume measurements of the ionosphere-thermosphere-magnetosphere system in response to changing solar wind conditions. This toolset is currently being extended to include data from the SuperDARN HF radar network, GPS scintillation sensors in the polar cap, and Fabry-Perot Interferometer (FPI) measurements of the neutral wind field. The high-level data products produced through this data fusion approach can be directly applied as constraints for regional and global models of the geospace system, improving space weather predictive capabilities.

2 Guiding Objectives of this Research

This research project was guided by two key questions:

1. **How is F-region plasma structure modified during polar cap transit?**
The relative contributions of transport, precipitation, recombination, field-aligned currents, and thermal diffusion in controlling plasma structures in the polar cap remains poorly understood. A major impediment has been the lack of diagnostic measurements able to provide the requisite three-dimensional view of the evolving ionospheric state. The electronically steerable Advanced Modular ISR (AMISR) sensors fill this need by allowing acquisition of information in multiple directions simultaneously. Using common volume observations by RISR, PolarDARN, and an all-sky spectral imaging system, we have carried out the first quantitative and experimentally verified calculation of three-dimensional plasma continuity at the geomagnetic pole [*Dahlgren et al.*, 2012a; *Perry et al.*, 2015; *Semeter et al.*, 2014].

2. **How do magnetospheric drivers alter ionospheric composition, and what are the global implications?**
The topside polar ionosphere serves as a significant reservoir of magnetospheric ions. During disturbed conditions, precipitation, frictional heating, and field aligned currents act to modify F-region ion composition, converting the ionosphere from predominantly atomic (O^+) to predominantly molecular (NO^+). But no systematic methodology has yet been developed to quantify this effect through ground-based measurements. Progress on this question has come in the form of clarifying the location and rate of energy deposition in the F-region and topside ionosphere [*Akbari et al.*, 2015; *Akbari and Semeter*, 2014], and developing a mathematical framework through which produce sufficient observational constraints to access composition information reliably [*Semeter and Zettergren*, 2014; *Swoboda et al.*, 2015]

3 Project publications

Seven peer-reviewed papers were supported by this project and acknowledge AFOSR support under this grant, as listed below. These papers were also presented at international conferences (AGU, CEDAR, GEM, URSI) during the course of this project. In the remainder of this report we provide a synoptic overview of the major findings reported in this body of work.

1) Dahlgren, H., G. W. Perry, J. L. Semeter, J.-P. St.-Maurice, K. Hosokawa, M. J. Nicolls, M. Greffen, K. Shiokawa, and C. Heinselman, Space-time variability of polar cap patches: Direct evidence for internal plasma structuring, *Journal of Geophysical Research (Space Physics)*, *117*, A09312, doi: 10.1029/2012JA017961, 2012.

2) Semeter, J., and M. Zettergren, Model-Based Inversion of Auroral Processes, in *Modeling the Ionosphere-Thermosphere System*, edited by J. Huba, R. Schunk, and G. Khazanov, John Wiley & Sons, Ltd, Chichester, UK, doi: 10.1002/9781118704417.ch25, 2014.

3) Akbari, H., and J. L. Semeter, Aspect angle dependence of naturally enhanced ion acoustic lines, *Journal of Geophysical Research (Space Physics)*, *119*, 5909–5917, doi: 10.1002/2014JA019835, 2014.

4) Akbari, H., J. L. Semeter, M. A. Hirsch, P. Guio, and M. J. Nicolls, Evidence for generation of unstable suprathermal electron population in the auroral F region, *Geophys. Res. Lett.*, *42*, 185–192, doi: 10.1002/2014GL062598, 2015.

5) Swoboda, J., J. Semeter, and P. Erickson, Space-Time Ambiguity Functions for Electronically Scanned ISR Applications, *Rad. Sci.*, *50*, doi: 10.1002/2014RS005620, 2015.

6) Perry, G., et al., Spatiotemporally resolved electrodynamic propertiesof a sun-aligned arc over Resolute Bay, *Geophys. Res. Lett.*, *42*, in press, 2015.

7) Semeter, J., H. Dahlgren, M. Zettergren, J. Swoboda, G. Perry, J.-P. St.-Maurice, K. Hosokawa, K. Shiokawa, and M. Nicolls, Extreme F-region gradients generated by patch-arc interactions in the polar cap, *AGU Fall Meeting Abstracts*, pp. SA24A–07, 2014 (Invited).

4 Research Accomplishments

This section highlights published results from the project. The results are organized into three categories: (i) results derived from radar-optical sensor Fusion, (ii) optimal experiment design approaches developed in support of these investigations, and (iii) F-region turbulence as a "hidden" term in ionospheric energy balance. In each category, a synoptic overview of the results are presented. For further details, see the full journal articles.

4.1 ISR-SuperDARN-Optical sensor fusion

Using the RISR facility, *Dahlgren et al.* [2012a] published the first direct three-dimensional time-dependent measurements of a transiting polar plasma patch. Figure 1 shows an example composite image. The plasma density slices at 340 km, 250 km and the vertical slice are produced by extracting cuts of the trilinear interpolation of RISR multi-beam measurements. The positions of the radar beams are marked on each horizontal slice as black circles (this method of RISR visualization has been previously discussed by [*Dahlgren et al.*, 2012b]). The structure has a peak electron density of $1.5 \times 10^11\text{m}^{-3}$, close to 250 km in altitude. The contemporary 630.0 nm allsky camera image is magnetically mapped to 200 km altitude for display purposes (the actual emission is closer to 250km). The emission ratio brightness of signal over average background is given by the horizontal color bar at the bottom of the figure. The optical enhancements correspond to the location of the plasma structures seen in the radar data. The coherent scatter from the SuperDARN radar is then plotted at 300 km altitude. The strongest echo (up to 30 dB, color bar to the left in the figure) comes from the region to the north-east of the vertical slice, partially overlapping the RISR-N plasma structure.

Perry et al. [2015] extended this experimental approach to investigate relationship between optical forms and derived electrodynamic parameters, in an effort to capture a full electrodynamic view of magnetosphere-ionosphere interactions during the formation of a plasma patch near the poleward auroral boundary. Figure 2 shows an example result from this work. Estimates of $|E_\perp|$ with vectors indicating the direction of the field, and $J_{||}$ are plotted along with 630-nm allsky camera data. The altitude of the contours for plasma density (Ne), ion temperature (Ti), Pedersen conductance ($\sum_P$), and $J_{||}$ are centered at 325 km. The $\sum_P$ estimates are a product of integrating the Pedersen conductivities between 200 and 500 km altitude along the magnetic field. The $|E_\perp|$ contours are

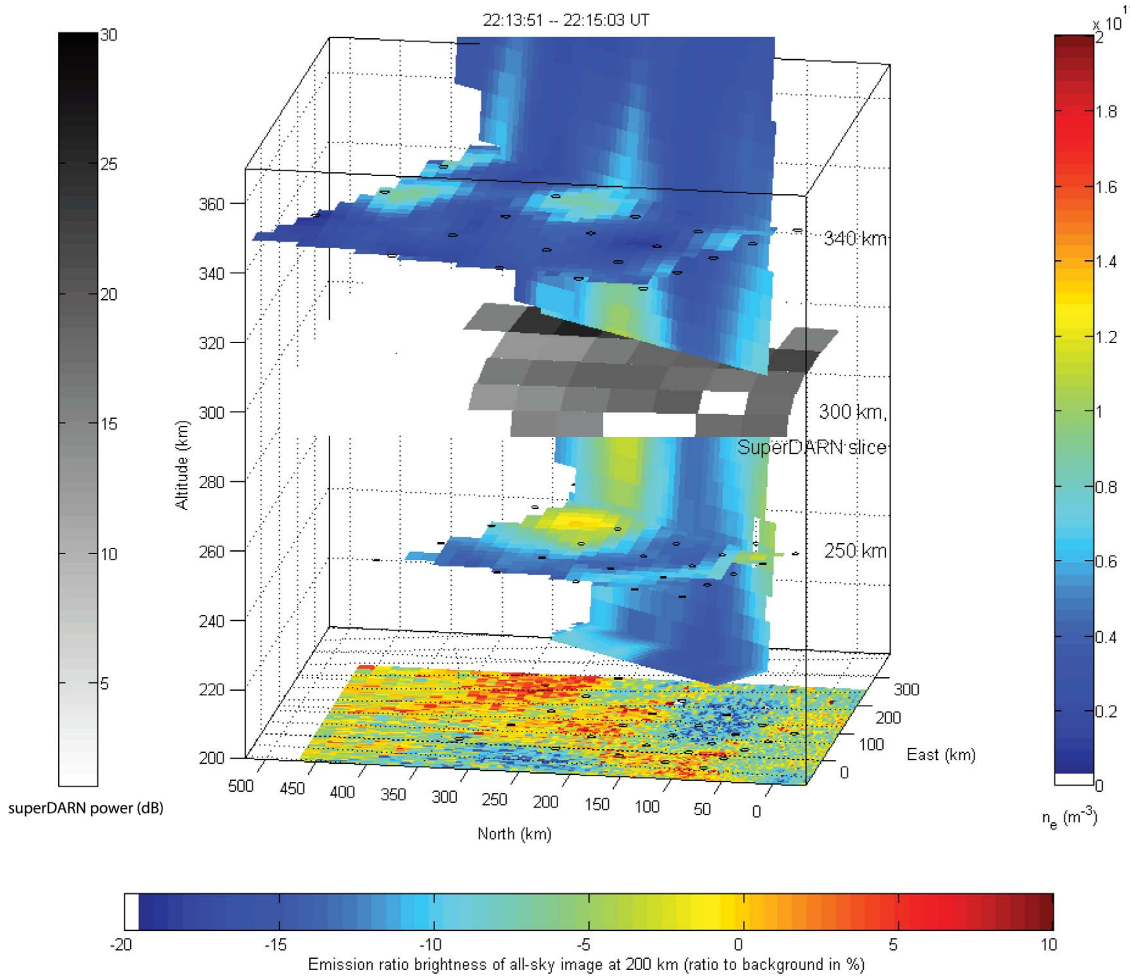

Figure 1: Three-dimensional view of an F region plasma density structure. The slices at 350 km and 250 km as well as the vertical slice show the electron density as derived from RISR-N data. The location of the radar beams are marked as black circles on the horizontal slices. At 300 km altitude, the Super- DARN echo is shown. The simultaneous 630.0 nm allsky image is projected to 200 km altitude, for which the emission brightness over the background level is indicated with the color bar below the combined plot. Optical signatures are seen in the location of plasma density enhancements, whereas the coherent echo from SuperDARN is strongest to the side of the plasma structure. [From **?**]

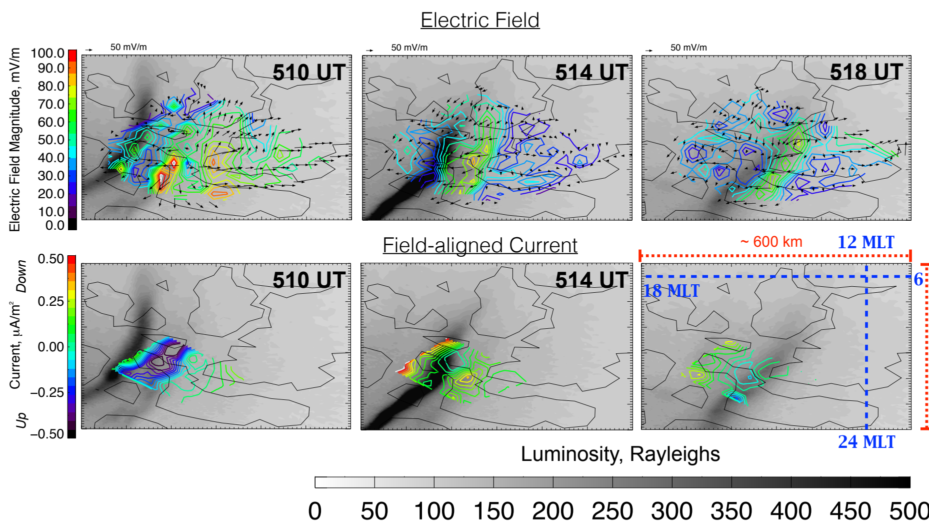

Figure 2: Combined plots of 630-nm allsky camera data (grayscale) and RISR contours for $|E_\perp|$ with corresponding vectors (top row), and $J_\parallel$ (bottom row). Dimensions of the field-of-view and MLT meridians are indicated in red and blue, respectively. [From *Perry et al.*, 2015]

constructed from data integrated over several hundred kilometres in altitude and mapped to 300 km altitude. The allsky data is mapped to 250 km altitude, the usual practice for 630.0 nm emissions.

Structuring in $|E_\perp|$ due to both arcs is significant and easily identifiable in this figure. Between 05:10 and 05:18 UT, meridionally extended $|E_\perp|$ structures moved towards dawn, coincident with the two optical arcs discussed earlier. At 05:10 UT, three structures with low —E— were in the FOV. Two of the structures, both with $|E_\perp|$ of ∼25 mV/m, were collocated with two optical arcs shown in grayscale. The low $|E_\perp|$ structures are indicative of the upward $J_\parallel$ region of an arc; a region of electron precipitation in which plasma production is enhanced, increasing the ionospheric conductivities. With enhanced conductivities $|E_\perp|$ decreases to uphold current closure. The upward $J_\parallel$ associated with the low $|E_\perp|$ structure of the brightest of the arcs is estimated to be approximately 0.5 μA/m^2, and maintains its intensity during the transit of the arc through the RISR FOV.

Semeter et al. [2014] used similar RISR experimental modes to focus on the interaction of plasma density patches and auroral processes. Figure 3 shows three frames of this time-dependent dynamic. The color contours are a vertical meridional representation of plasma density. The auroral images are displayed as flat perpendicular gray scale images. The red dashed line indicates the projection of the density cut into the allsky frame. These results suggested a time- steepening of F-region density gradients within a downward field-aligned current channel. The evacuating region was sandwiched in between a nascent sun-aligned arc and a plasma patch, indicating a mechanism of structuring via plasma removal. The challenge in quantifying this result lies in dealing with sampling issues associated with the limited number of radar beams and limited integration period used to construct the density images. Future work that fuses these measurements with 3-D physics-based modeling will contribute to clarifying this result.

The sensor fusion approach exemplified in these results represents a path forward for extracting

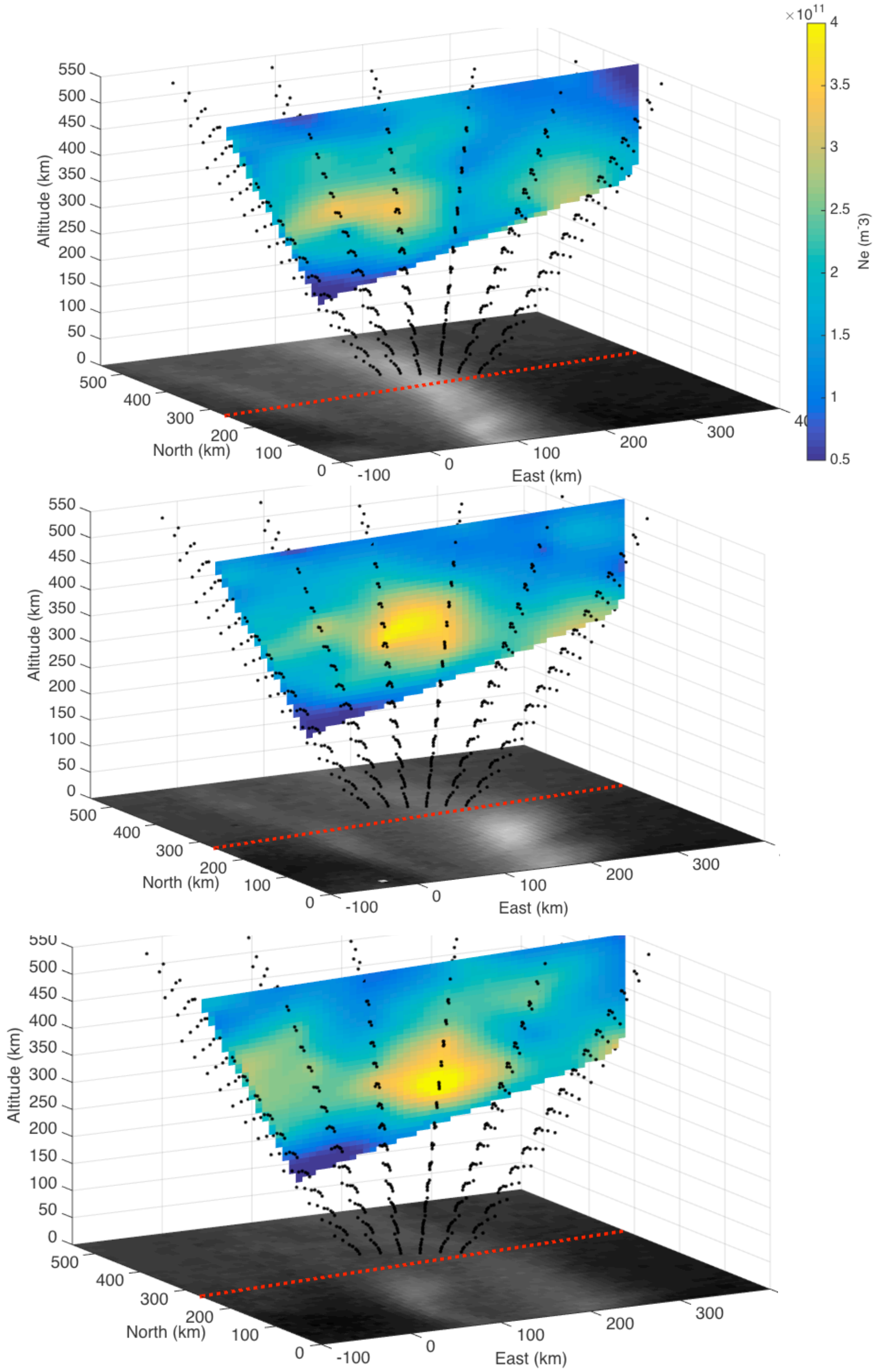

Figure 3: Snapshots of vertical meridional cuts through a plasma density structure in the polar cap (color contours) as rendered from RISR samples (black dots). These are overlain on on horizontal maps of 630-nm brightness (gray scale) observed by the collocated allsky camera. The red dashed line indicates the projection of the density cut into the camera frame. The figure illustrates an evolving plasma patch sandwiched between two polar cap arcs. [From *Semeter et al.*, 2014]

optimal constraints on polar ionospheric dynamics. Such fused data products can be repackaged in a variety of formats, which can then provide valuable quantitative constraints for first-principles physical modeling efforts. As part of this effort, a mathematical framework and flexible software package have been developed in beta form, with the goal of providing such a tool to the modeling community. Activity on this effort is discussed in the following section.

4.2 Optimal experiment design for electronically steerable ISR

The aforementioned experimental results applied standard interpolation and mapping strategies, without the use of any physical knowledge of how the parameters should be connected or what spatiotemporal variations are allowed under known physics. An inverse-theoretic framework for incorporating physics knowledge into the analysis was developed by [*Semeter and Zettergren*, 2014] under this project. A schematic overview of the approach is shown in Figure 4. The basic approach is to develop parallel forward models between the magnetospheric drivers and the ionospheric response (both optical and ISR) which is subsequently inverted using Bayesian techniques. The Bayesian approach allows for incorporating uncertainties in model assumptions and tracking how they impact the results.

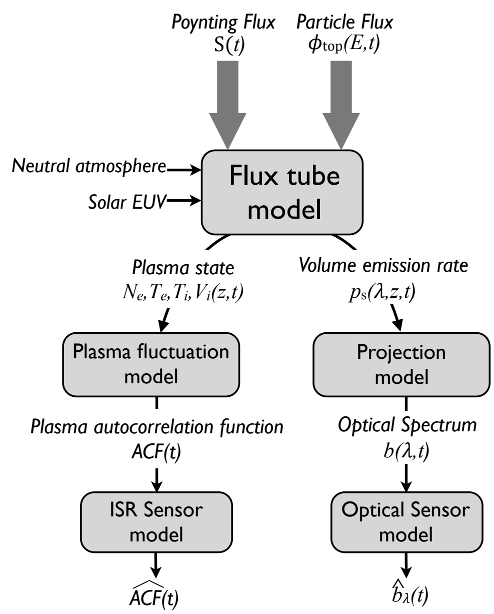

Figure 4: Schematic representation of the forward problem treated by [*Semeter and Zettergren*, 2014]. A flux of incident electrons ϕ_{top} impinges the atmosphere, which heats, ionizes, and excites the neutral gases. These rates are collectively represented by $p(x, y)$. A physical flux-tube model maps these inputs to changes in the ionosopheric state and optical emission rates. State parameters (left side) are sensed as changes in the plasma autocorrelation function measured by ISR, optical emissions (right side) are sensed as brightness variations in a camera system. This data flow describes a forward model, which may be reversed to reconstruct the magnetospheric drivers, in this case ϕ_{top}). [From *Semeter and Zettergren*, 2014]

A second track to improving sensor resolution was pursued by *Swoboda et al.* [2015], who exploited the unique multi-beam capability of RISR to deal with motion of the ionospheric target during the data acquisition period. Their approach developed the concept of a three-dimensional ISR ambiguity function. The essential idea is captured by considering a fixed ionospheric pattern moving through a field that is being sampled by a regular grid of radar beams. ISR backscatter is a stochastic process, and so time-integration is required to estimate the plasma parameters. If a plasma parcel moves into an adjacent beam during this integration period, then we have a classic blurring problem, where echoes from multiple beams could be combined to improve fidelity. This notion is capture in Figure 5

4.3 Langmuir turbulence: A hidden energy transfer mechanism

In addition to macro-scale (fluid) instabilities, such as gradient-drift and shear-driven, particle fluxes and field-aligned currents also produce micro-scale (kinetic) instabilities—e.g., unstable Langmuir waves which couple to other modes. These effects are manifested in ISR observations as enhanced non-thermal backscatter, sometimes known as "Naturally Enhanced Ion-Acoustic Lines" or NEIALs. [*Akbari et al.*, 2015] used PFISR to establish the geospatial context of these scattering events, suggesting an intriguing correlation with ground-based observation of "MF bursts". [*Akbari and Semeter*, 2014] used the unique electronic steering capabilities of PFISR to observed the dependence of NEIALs on magnetic aspect angle.

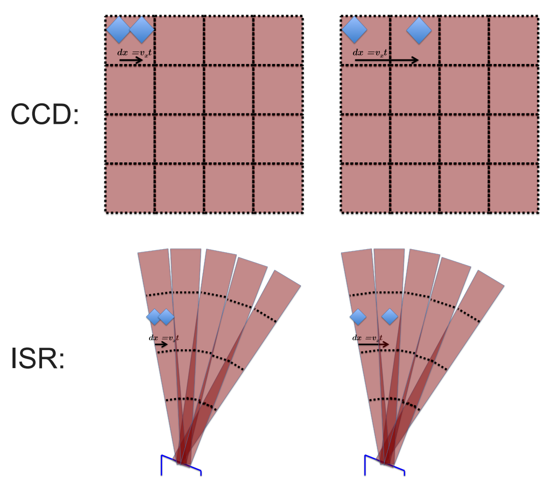

Figure 5: Illustration of digital blurring for a CCD focal plane (top) and for a set of ISR beams (right). Electronically steerable ISR is able to integrate in an effectively simultaneous manner in multiple beams, thus enabling integration across multiple beams as the plasma target moves. This framework has a strong analogy to deblurring in optical imagery. [From *Swoboda et al.*, 2015]

These results suggested that Langmuir turbulence may represent a "hidden" mode of energy transfer in the high-latitude F-region, which has direct effect on the structuring and composition objectives of this research. Exploration along these lines has lead to experimental modes able to isolate with unprecedented resolution the relationship between these instabilities to the bulk properties of the ionosphere. Figure 6 exemplifies this result. Enhanced UHF backscatter at 100-150 km is caused by the usual auroral energy deposition mechanism, namely, impact ionization of the neutral gases. But the enhanced echoes at 200-300 km are related to Langmuir turbulence produced by collisionless energy deposition in the low-energy regime of the impinging electron spectrum. The process is expected to occur broadly throughout the disturbed high-latitude geospace system. The significance of this latter energy deposition process to the structure and composition of the ionosphere is not known.

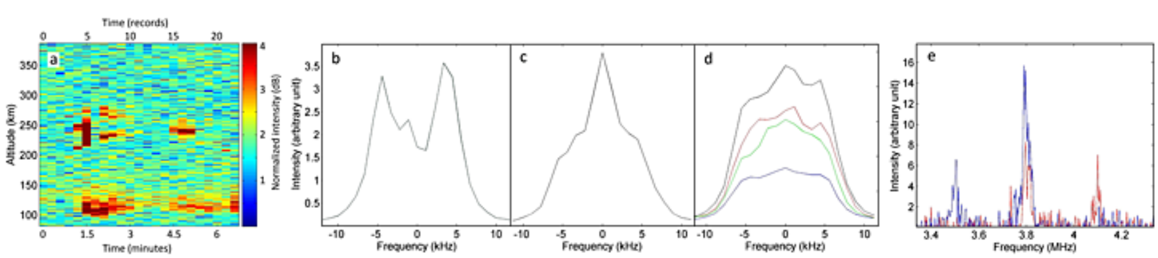

Figure 6: (a) Ion line range-time-intensity (RTI) plot derived from a separate 1 baud length pulse that accompanied AC. The time axis is shown in minutes as well as in 16 s intervals (records). Coherent echoes are originating from thin layers close to the F-region peak (∼250 km). (b–d) Examples of ion line spectra measured from the turbulence layers. Each spectrum corresponds to different times. (e) Up- (blue) and down-shifted (red) plasma line spectra produced by long-pulse measurements for record 16 in panel a. The spectra are averaged over a 70 km range gate centered at 290 km. [From *Akbari et al.*, 2015]

References

Akbari, H., and J. L. Semeter, Aspect angle dependence of naturally enhanced ion acoustic lines, *Journal of Geophysical Research (Space Physics)*, *119*, 5909–5917, doi: 10.1002/2014JA019835, 2014.

Akbari, H., J. L. Semeter, M. A. Hirsch, P. Guio, and M. J. Nicolls, Evidence for generation of unstable suprathermal electron population in the auroral F region, *Geophys. Res. Lett.*, *42*, 185–192, doi: 10.1002/2014GL062598, 2015.

Basu, S., and C. Valladares, Global aspects of plasma structures, *J. Atmos. Sol. Terr. Phys.*, *61*, 127–139, doi: 10.1016/S1364-6826(98)00122-9, 1999.

Brambles, O. J., W. Lotko, B. Zhang, M. Wiltberger, J. Lyon, and R. J. Strangeway, Magnetosphere Sawtooth Oscillations Induced by Ionospheric Outflow, *Science*, *332*, 1183–, doi: 10.1126/science.1202869, 2011.

Chappell, C. R., T. E. Moore, and J. H. Waite Jr., The ionosphere as a fully adequate source of plasma for the Earth's magnetosphere, *J. Geophys. Res.*, *77*, 6104, 1987.

Dahlgren, H., G. W. Perry, J. L. Semeter, J.-P. St.-Maurice, K. Hosokawa, M. J. Nicolls, M. Greffen, K. Shiokawa, and C. Heinselman, Space-time variability of polar cap patches: Direct evidence for internal plasma structuring, *Journal of Geophysical Research (Space Physics)*, *117*, A09312, doi: 10.1029/2012JA017961, 2012a.

Dahlgren, H., J. L. Semeter, K. Hosokawa, M. J. Nicolls, T. W. Butler, M. G. Johnsen, K. Shiokawa, and C. Heinselman, Direct three-dimensional imaging of polar ionospheric structures with the Resolute Bay Incoherent Scatter Radar, *Geophys. Res. Lett.*, *39*, L05104, doi: 10.1029/2012GL050895, 2012b.

Perry, G., et al., Spatiotemporally resolved electrodynamic propertiesof a sun-aligned arc over Resolute Bay, *Geophys. Res. Lett.*, *42*, In press, 2015.

Schunk, R. W., Theoretical developments on the causes of ionospheric outflow, *J. Atmos. Sol. Terr. Phys.*, *62*, 399–420, doi: 10.1016/S1364-6826(00)00017-1, 2000.

Semeter, J., and M. Zettergren, Model-Based Inversion of Auroral Processes, in *Modeling the Ionosphere-Thermosphere System*, edited by J. Huba, R. Schunk, and G. Khazanov, John Wiley & Sons, Ltd, Chichester, UK, doi: 10.1002/9781118704417.ch25, 2014.

Semeter, J., H. Dahlgren, M. Zettergren, J. Swoboda, G. Perry, J.-P. St.-Maurice, K. Hosokawa, K. Shiokawa, and M. Nicolls, Extreme F-region gradients generated by patch-arc interactions in the polar cap, *AGU Fall Meeting Abstracts*, pp. SA24A–07, 2014.

Swoboda, J., J. Semeter, and P. Erickson, Space-Time Ambiguity Functions for Electronically Scanned ISR Applications, *Rad. Sci.*, *50*, doi: 10.1002/2014RS005620, 2015.

1.

1. Report Type

Final Report

Primary Contact E-mail
Contact email if there is a problem with the report.

jls@bu.edu

Primary Contact Phone Number
Contact phone number if there is a problem with the report

6173583498

Organization / Institution name

Boston University

Grant/Contract Title
The full title of the funded effort.

Magnetospheric control of density and composition in the polar ionosphere

Grant/Contract Number
AFOSR assigned control number. It must begin with "FA9550" or "F49620" or "FA2386".

FA9550-12-1-0184

Principal Investigator Name
The full name of the principal investigator on the grant or contract.

Joshua Semeter

Program Manager
The AFOSR Program Manager currently assigned to the award

Kent Miller

Reporting Period Start Date

04/01/2012

Reporting Period End Date

03/31/2015

Abstract

At high magnetic latitudes, the ionosphere, thermosphere, and magnetosphere respond in a coherent fashion to variations in the impinging solar wind. Understanding the origin of structure, composition, and motions in the polar ionosphere requires distributed heterogeneous measurements and a systems approach. This research has used collaborative observations by UHF incoherent scatter radar (ISR), the SuperDARN HF radar network, and wide-angle monochromatic optical imagers, supported by first-principles numerical modeling, to investigate the driving mechanisms and technological implications of these interactions. Key observational evidence has been provided by the electronically steerable Incoherent Scatter Radar at Resolute Bay, Canada. The findings of this research, published in a series of papers, include both technical contributions related to the application of phased array ISR in the deep polar cap, and scientific contributions arising from the application of these techniques. Specific results include: 1) Development of a sensor fusion framework for combining simultaneous observations of auroral phenomena observed by radar and optical means [Semeter and Zettergren, 2014], 2) Development of a deconvolution approach for analyzing volumetric ISR measurements in a temporally and spatially varying ionosphere [Swoboda et al., 2015], 3) Discovery of direct evidence for internal structuring of convecting plasma patches [Dahlgren et al., 2013], 4) Quantitative description of electrodynamic coupling within polar auroral arcs developing along the nightside polar cap boundary [Perry et al., 2015], 5) Steepening of

ionospheric density gradients via magnetosphere-ionosphere coupling at the poleward auroral boundary, and 6) Measurements of anomalous ion heating by Langmuir turbulence caused be soft particle fluxes in the aurora -- a possible ``hidden" energy source for F-region energy balance at high latitudes [Akbari et al., 2014, 2015].

Distribution Statement

This is block 12 on the SF298 form.

Distribution A - Approved for Public Release

Explanation for Distribution Statement

If this is not approved for public release, please provide a short explanation. E.g., contains proprietary information.

SF298 Form

Please attach your SF298 form. A blank SF298 can be found here. Please do not password protect or secure the PDF The maximum file size for an SF298 is 50MB.

AFD-070820-035_js copy_js.pdf

Upload the Report Document. File must be a PDF. Please do not password protect or secure the PDF . The maximum file size for the Report Document is 50MB.

AFOSR_2015_FinalReport.pdf

Upload a Report Document, if any. The maximum file size for the Report Document is 50MB.

Archival Publications (published) during reporting period:

1) Dahlgren, H., G. W. Perry, J. L. Semeter, J.-P. St.-Maurice, K. Hosokawa, M. J. Nicolls, M. Greffen, K. Shiokawa, and C. Heinselman, Space-time variability of polar cap patches: Direct evidence for internal plasma structuring, Journal of Geophysical Research (Space Physics), 117, A09312, doi: 10.1029/2012JA017961, 2012.

2) Semeter, J., and M. Zettergren, Model-Based Inversion of Auroral Processes, in Modeling the Ionosphere-Thermosphere System, edited by J. Huba, R. Schunk, and G. Khazanov, John Wiley & Sons, Ltd, Chichester, UK, doi: 10.1002/9781118704417.ch25, 2014.

3) Akbari, H., and J. L. Semeter, Aspect angle dependence of naturally enhanced ion acoustic lines, Journal of Geophysical Research (Space Physics), 119, 5909–5917, doi: 10.1002/2014JA019835, 2014.

4) Akbari, H., J. L. Semeter, M. A. Hirsch, P. Guio, and M. J. Nicolls, Evidence for generation of unstable suprathermal electron population in the auroral F region, Geophys. Res. Lett., 42, 185–192, doi: 10.1002/2014GL062598, 2015.

5) Swoboda,J.,J.Semeter,andP.Erickson,Space-TimeAmbiguityFunctionsforElectronically Scanned ISR Applications, Rad. Sci., 50, doi: 10.1002/2014RS005620, 2015.

6) Perry,G.,etal.,Spatiotemporallyresolvedelectrodynamicpropertiesofasun-alignedarcover Resolute Bay, Geophys. Res. Lett., 42, in press, 2015.

7) Semeter, J., H. Dahlgren, M. Zettergren, J. Swoboda, G. Perry, J.-P. St.-Maurice, K. Hosokawa, K. Shiokawa, and M. Nicolls, Extreme F-region gradients generated by patch- arc interactions in the polar cap, submitted March 2015 (presented as AGU Fall Meeting Abstracts, pp. SA24A–07, 2014).

Changes in research objectives (if any):

Change in AFOSR Program Manager, if any:

Extensions granted or milestones slipped, if any:

AFOSR LRIR Number

LRIR Title

Reporting Period

Laboratory Task Manager

Program Officer

Research Objectives

Technical Summary

Funding Summary by Cost Category (by FY, $K)

	Starting FY	FY+1	FY+2
Salary			
Equipment/Facilities			
Supplies			
Total			

Report Document

Report Document - Text Analysis

Report Document - Text Analysis

Appendix Documents

2. Thank You

E-mail user

Jun 13, 2015 14:03:45 Success: Email Sent to: jls@bu.edu